Figures and figure supplements

Alternative splicing at neuroligin site A regulates glycan interaction and synaptogenic activity

Shinichiro Oku *et al*

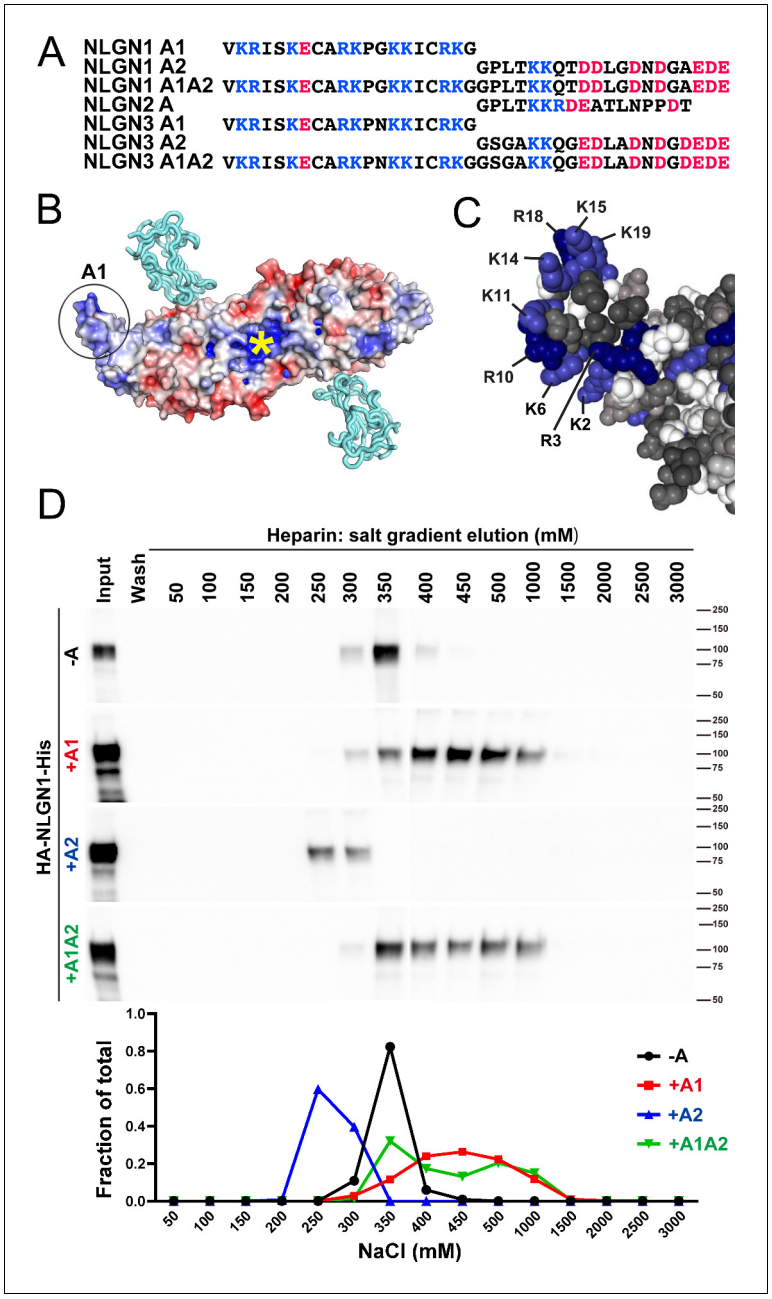

Figure 1. NLGN1 alternative splicing at site A regulates heparin/HS binding. (**A**) The amino acid sequences of each human NLGN A splice insert highlighting positively charged (blue) and negatively charged (red) residues. Splice insert sequences in mouse NLGN1-3 are identical to those in human NLGN1-3 except for one residue in NLGN1 A2 (7th residue H in mouse and Q in human). (**B**) Structure of the NLGN1-NRXN1β LNS domain complex (PDB: 3VKF) (***Tanaka et al., 2012***) showing the position of the A1 insert relative to the constitutive HS binding site (yellow asterisk) (***Zhang et al., 2018***). The NLGN1 surface is colored according to the electrostatic potential from blue (+8 kbT/ec) to red (−8 kbT/ec), and the NRXN LNS domain is in cyan. (**C**) Structure of the NLGN1 A1 splice insert (PDB: 3VKF) highlighting the positively charged surface residues proposed to participate in HS interaction. Residues are numbered from the beginning of the A1 insert. (**D**) Elution profile of purified recombinant NLGN1 isoform ectodomain proteins from a heparin column. Elution at a higher concentration of salt indicates stronger binding.

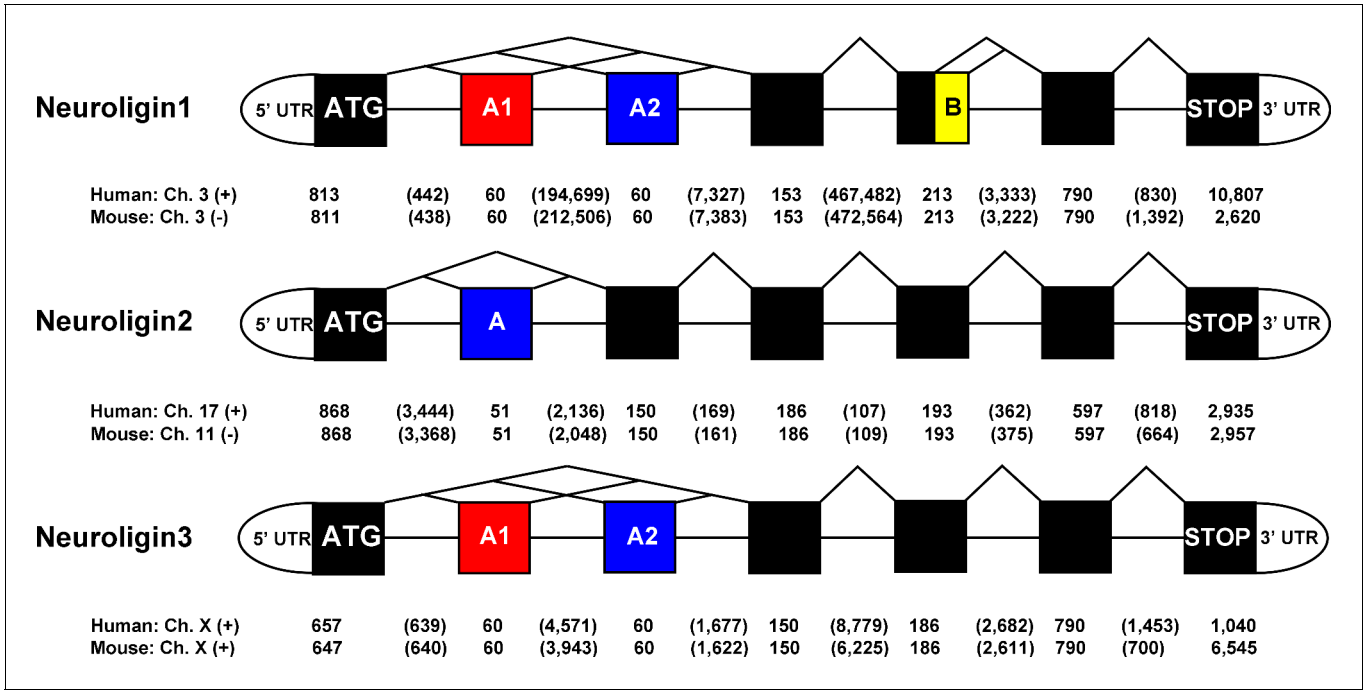

Figure 1—figure supplement 1. *NLGN* gene structures. Structure of the human and mouse *NLGN1-3* gene coding region highlighting alternatively spliced exons. Exon (boxes) and intron sizes are listed in base pairs.

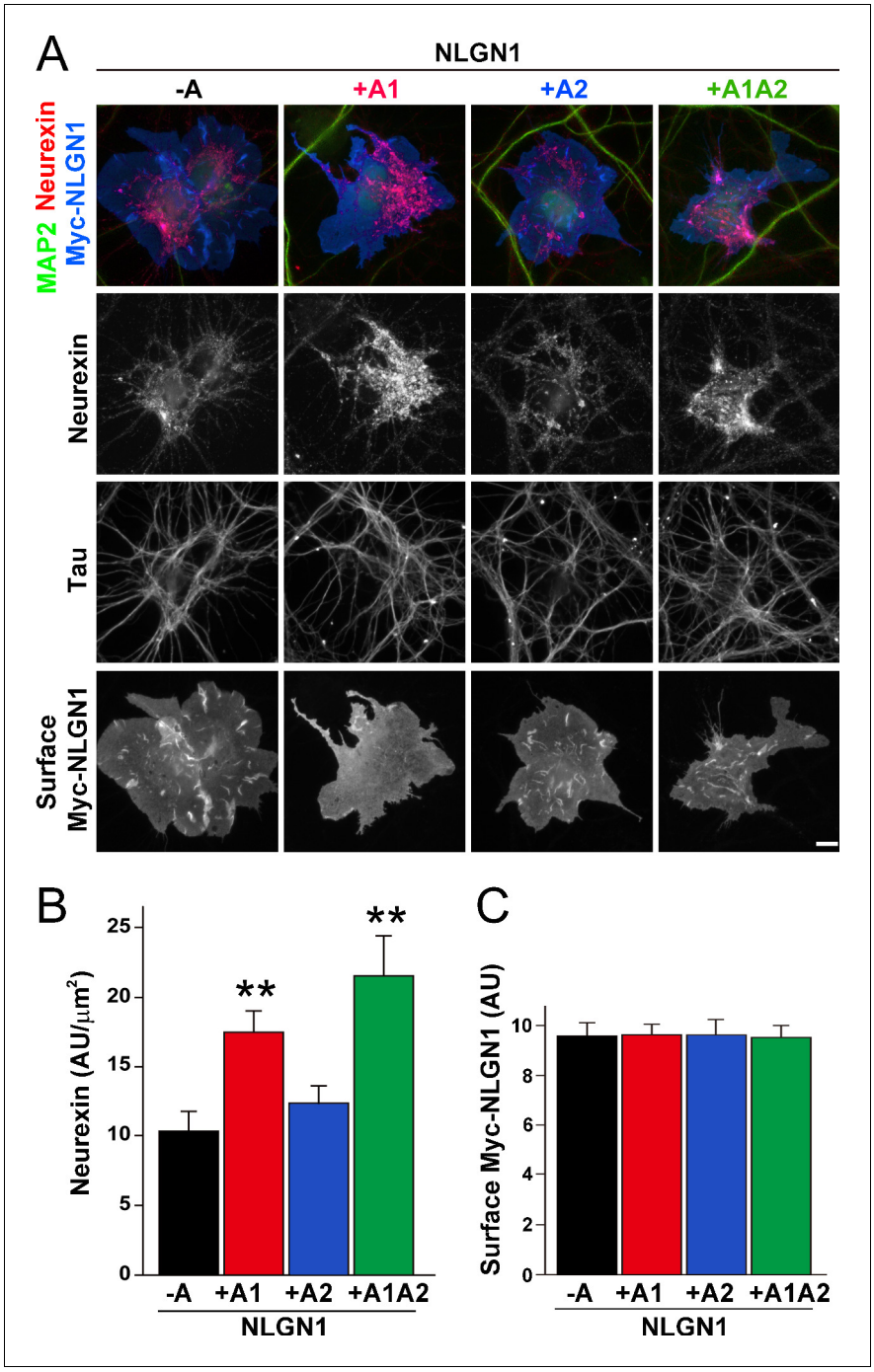

Figure 2. The NLGN1 A1 splice insert enhances neurexin recruitment in coculture. (**A–C**) Each NLGN1 isoform with an extracellular Myc tag was expressed in COS7 cells which were cocultured with hippocampal neurons. NLGN1 induced recruitment of neurexin along tau-positive axons. Axon regions contacting expressing COS7 cells and lacking contact with MAP2-positive dendrites were assessed to exclude native synapses. The total intensity of native neurexin (**B**) per contact area was normalized to a baseline value of 1 measured from sister cocultures performed with the negative control protein Myc-tagged Amigo. Neurexin recruitment differed among NLGN1 splice variants, $p<0.0005$ by Kruskal-Wallis test and $^{**}p<0.01$ compared with NLGN1 -A by post hoc Dunn's multiple comparisons test, n = 35–43 cells from four independent experiments. Although the value for NLGN1 +A1A2 was higher than that for NLGN1 +A1, this difference was not significant. COS7 cells were chosen for equal surface NLGN1 expression (**C**). Scale bar, 10 μm.

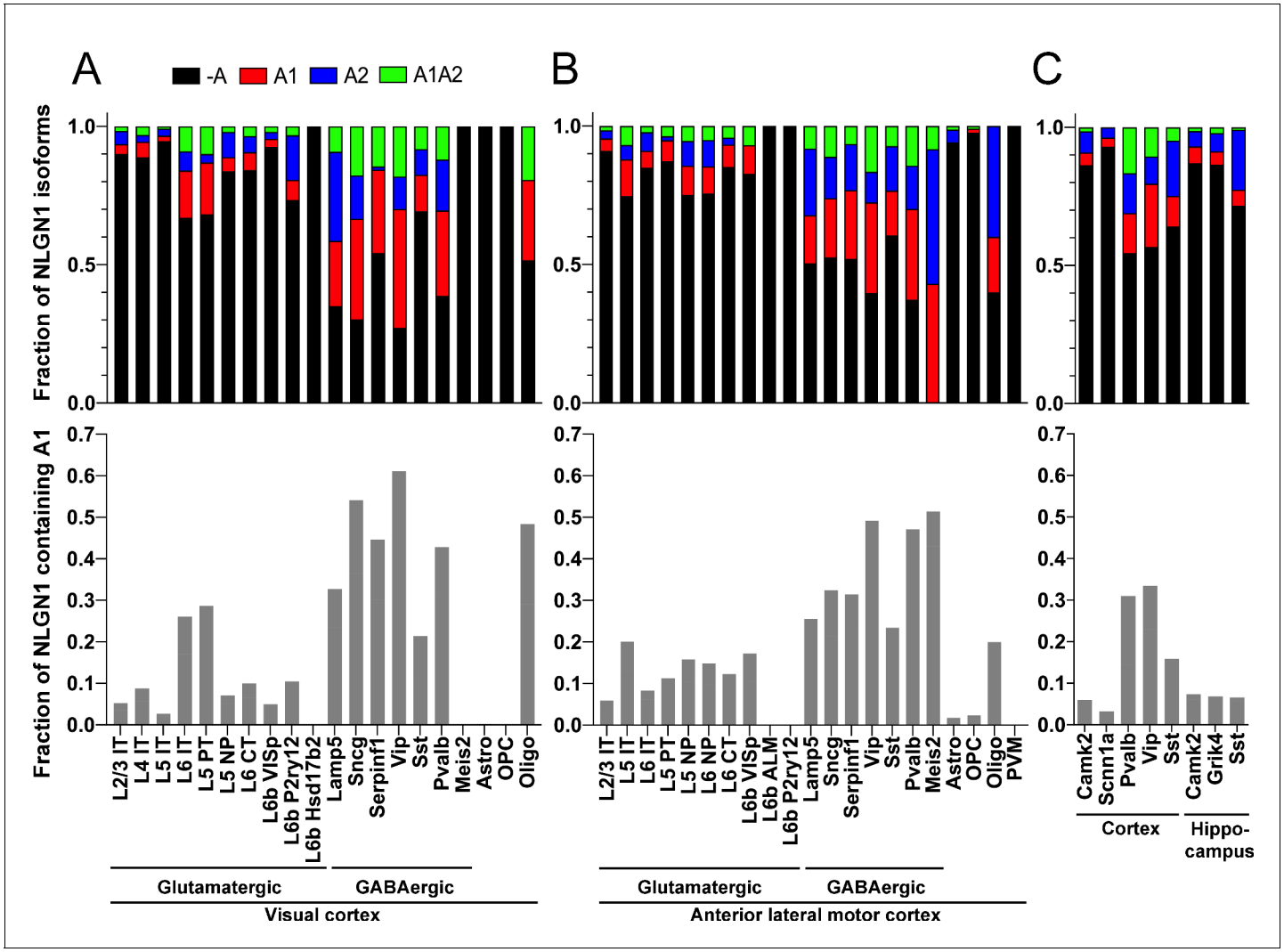

Figure 3. The NLGN1 A1 splice insert is high in GABAergic neuron cell types. The fraction of each mouse NLGN1 site A splice isoform transcript is plotted in each upper graph and the fraction of NLGN1 transcript that contains the A1 insert, that is (+A1 plus +A1A2)/total, is plotted in each lower graph. Datasets are from ***Tasic et al., 2018*** (A, B) and ***Furlanis et al., 2019*** (C).

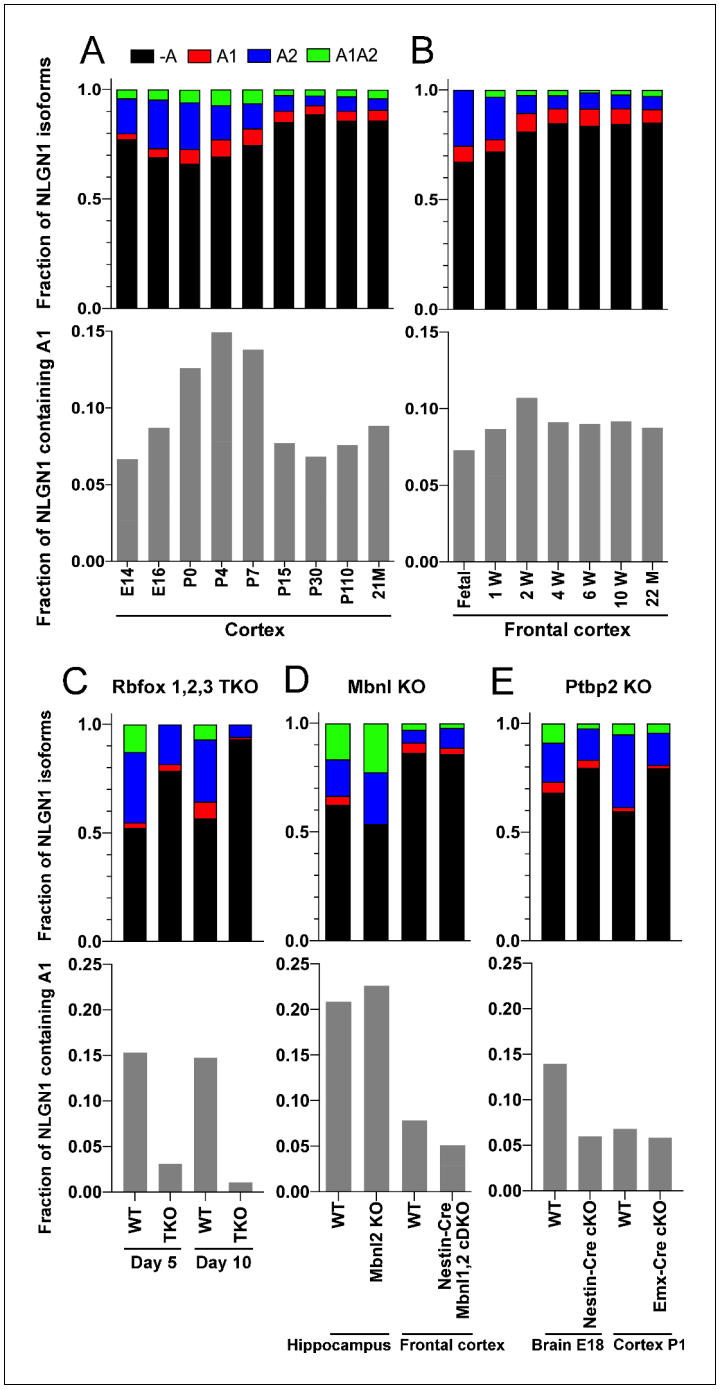

Figure 4. The NLGN1 A1 splice insert is regulated developmentally and by Rbfox splicing factors. The fraction of each mouse NLGN1 site A splice isoform transcript is plotted in each upper graph and the fraction of NLGN1 transcript that contains the A1 insert, that is (+A1 plus +A1A2)/total, is plotted in each lower graph. In the developmental studies (**A, B**), ages are indicated in embryonic (**E**) or postnatal (**P**) days, or in postnatal weeks (**W**) or months (**M**). Panel (**C**) data are from spinal neuron cultures differentiated from *Rbfox1,2,3* triple KO (TKO) embryonic stem cells and grown for the indicated number of days. Panel (**D**) data are from hippocampi from 2 to 3 month old *Mbnl2* KO mice or frontal cortex from adult $Mbnl1^{-/-}Mbnl2^{loxP/loxP}$ Nestin-Cre conditional double KO (cDKO) mice. Panel (**E**) data are from embryonic day 18 brain of $Ptbp2^{loxP/loxP}$ Nestin-Cre cKO mice or postnatal day 1 cortex of $Ptbp2^{loxP/loxP}$ Emx1-Cre cKO mice. Development datasets are from (**A**) (***Yan et al., 2015***) and (**B**) (***Lister et al., 2013***). Datasets from KO cells or mice lacking splice factors are from (**C**) (***Jacko et al., 2018***), (**D**) (***Charizanis et al., 2012***; ***Weyn-Vanhentenryck et al., 2018***) and (**E**) (***Li et al., 2014***).

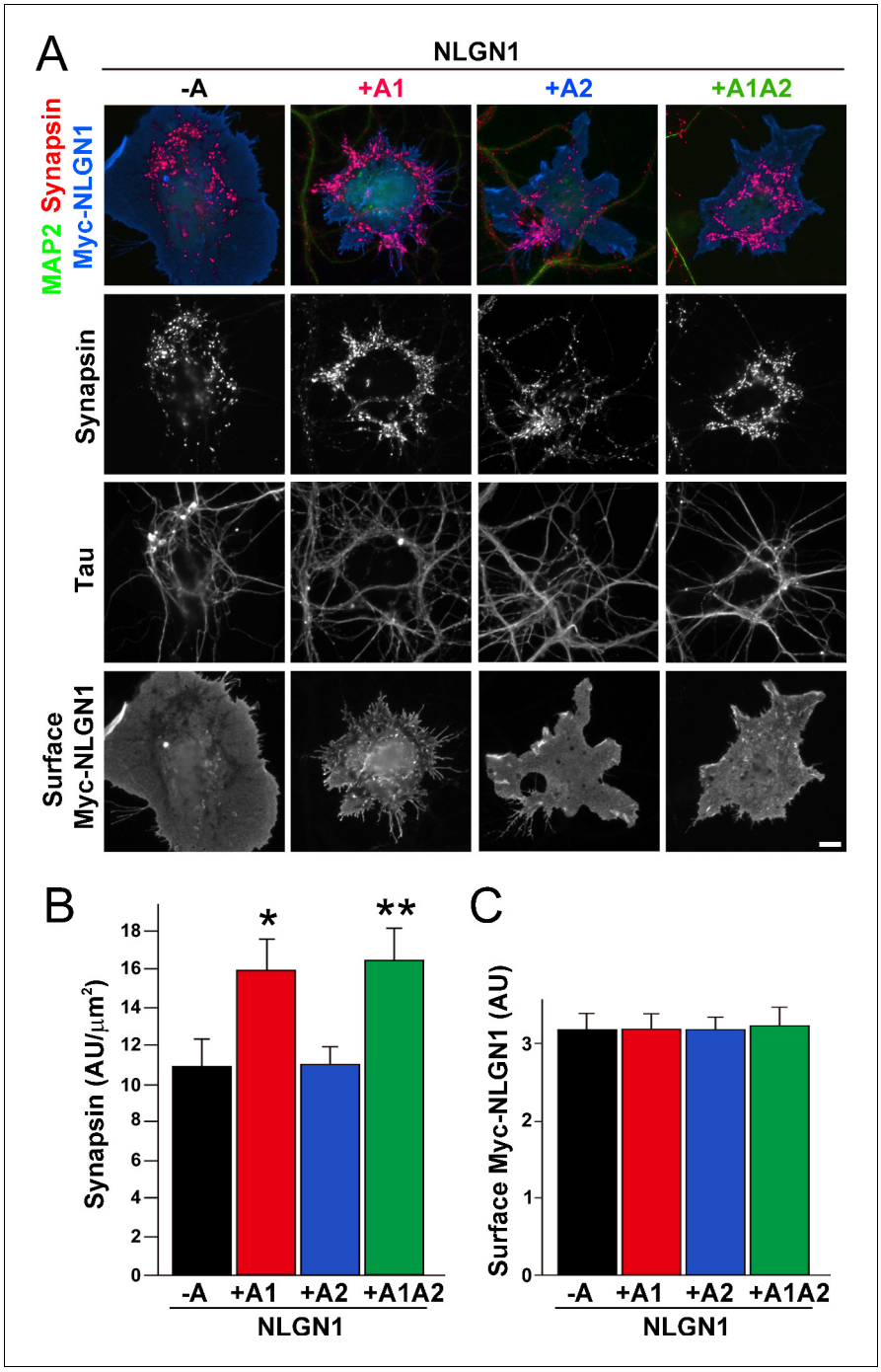

Figure 5. The NLGN1 A1 splice insert enhances presynaptic differentiation in coculture. (**A–C**) Each NLGN1 isoform with an extracellular Myc tag was expressed in COS7 cells which were cocultured with hippocampal neurons. NLGN1 induced clustering of synapsin along tau-positive axons. Axon regions contacting expressing COS7 cells and lacking contact with MAP2-positive dendrites were assessed to exclude native synapses. The total intensity of synapsin (**B**) per contact area was normalized to a baseline value of 1 measured from sister cocultures performed with the negative control protein Myc-tagged Amigo. Synapsin clustering differed among NLGN1 splice variants, $p<0.001$ by Kruskal-Wallis test and $^{*}p<0.05$ and $^{**}p<0.01$ compared with NLGN1 -A by post hoc Dunn's multiple comparisons test, n = 47–56 cells from four independent experiments. COS7 cells were chosen for equal surface Myc-NLGN1 expression (**C**). Scale bar, 10 μm.

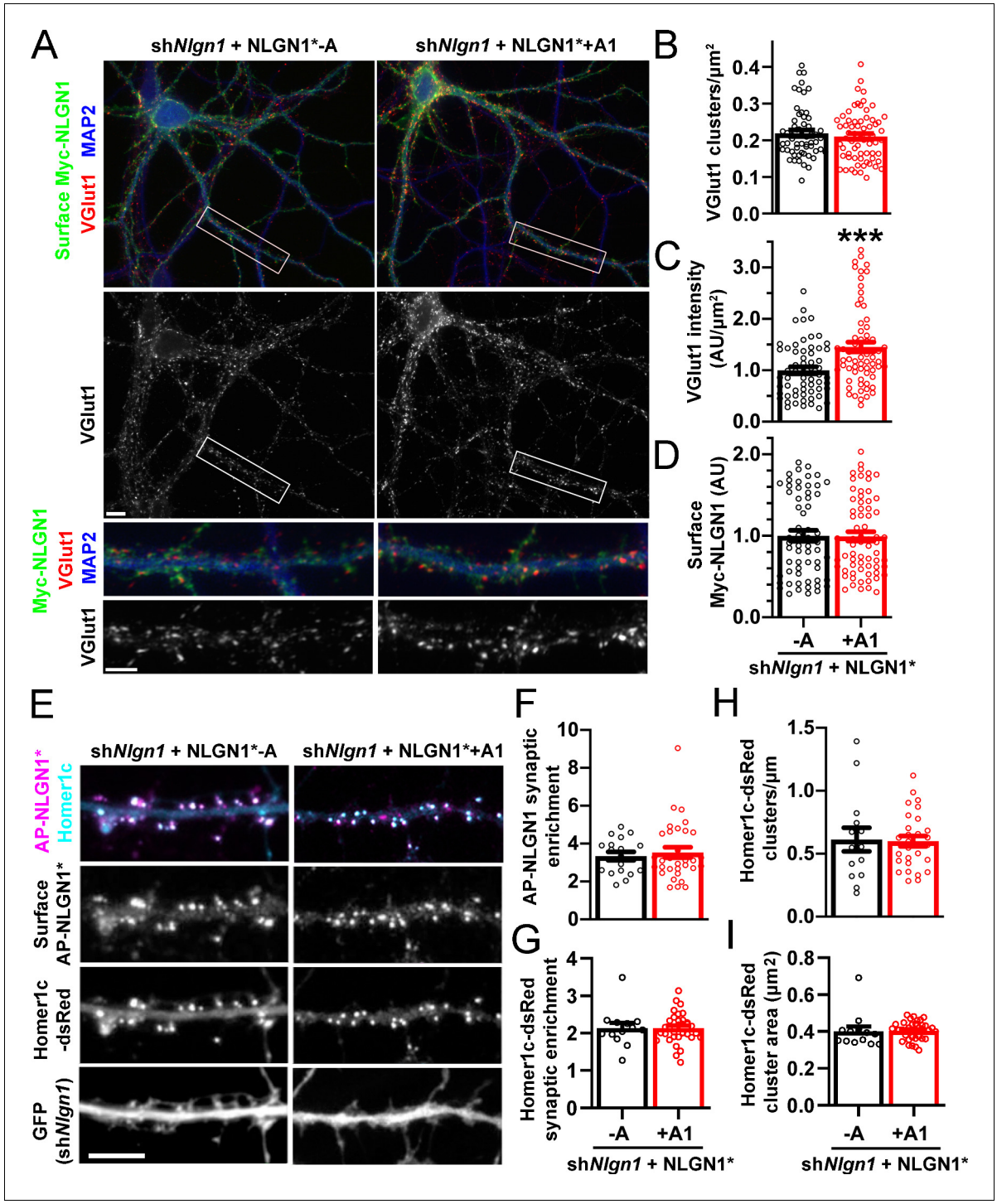

Figure 6. The NLGN1 A1 splice insert promotes structural synapse development. (**A–D**) Cultured hippocampal neurons were transfected with U6-sh*Nlgn1*-hSyn-CFP and hSyn-Myc-NLGN1* -A or +A1 at DIV 5 and neurons were fixed at DIV 12. The density of VGlut1 clusters did not differ but the total fluorescence intensity of VGlut1 inputs was higher for neurons expressing the NLGN1* +A1 than the -A isoform, ***p=0.0006 by Mann Whitney test, n = 59–66 neurons from three independent experiments. Cells were chosen for equal intensity of surface Myc-NLGN1. Scale bar, top 10 µm, bottom 5 µm. (**E–I**) Cultured hippocampal neurons were electroporated at plating with sh*Nlgn1*-GFP, Homer1c-dsRed, BirA^{ER}, and hSyn-AP-NLGN1* -A or +A1 and neurons imaged at DIV 14 following live cell labeling with streptavidin-Alexa647. The synaptic enrichment of AP-NLGN1*, defined as the intensity of AP-NLGN1* in Homer1c-dsRed-positive clusters relative to the intensity in the local dendrite shaft, did not differ between the splice variants, nor was there any difference in the synaptic enrichment or density or mean area of Homer1c-dsRed clusters (all p>0.1 by Mann Whitney test, n > 14 neurons from two independent experiments). Scale bar, 10 µm.

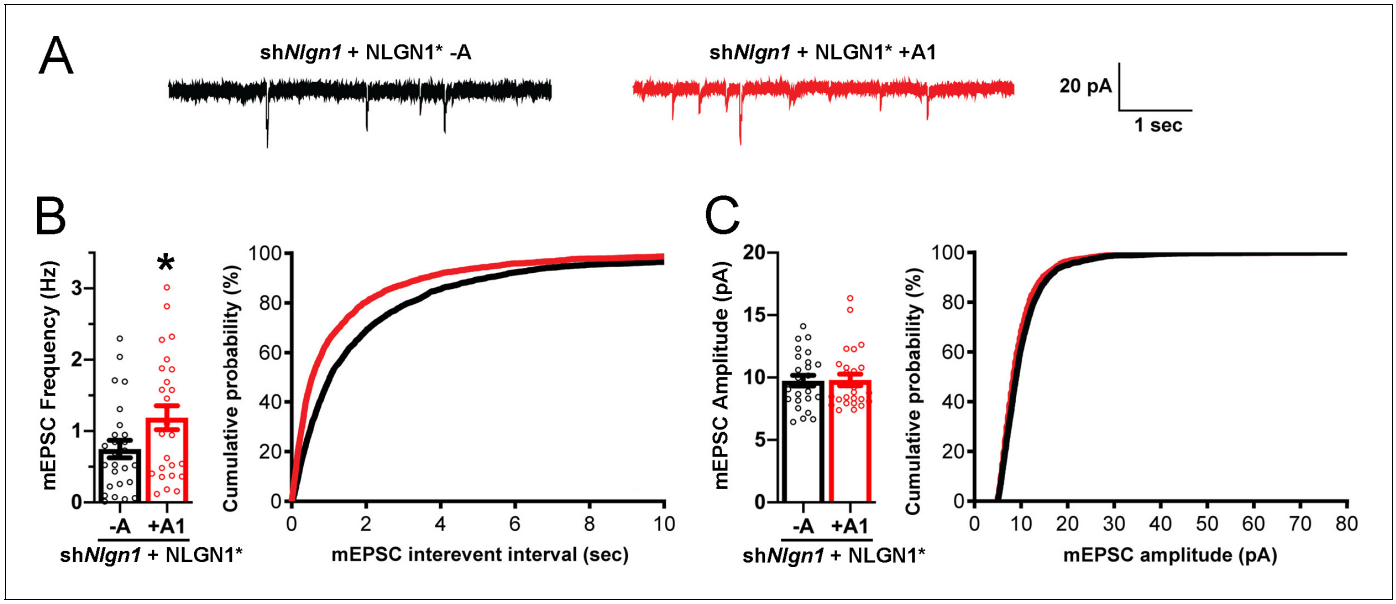

Figure 7. The NLGN1 A1 splice insert promotes functional synapse development. Cultured hippocampal neurons were transfected with U6-sh*Nlgn1*-hSyn-YFP, hSyn-DIO-YFP-P2A-HA-NLGN1* -A or +A1, and CAG-Cre at DIV 5. YFP positive neurons were selected for mEPSC recording at DIV 13 and 14. (**A**) Representative mEPSC traces from neurons expressing NLGN1* lacking (black trace) or containing (red trace) the A1 splice variant. (**B**) mEPSC frequency was significantly increased in NLGN1* +A1-expressing neurons (n = 26) relative to cells expressing NLGN1* -A (n = 26; *p=0.040 by Welch's t test), with a corresponding change in interevent interval. (**C**) mEPSC amplitude did not significantly differ between groups (p=0.93). Scale bar, 20 pA, 1 s.

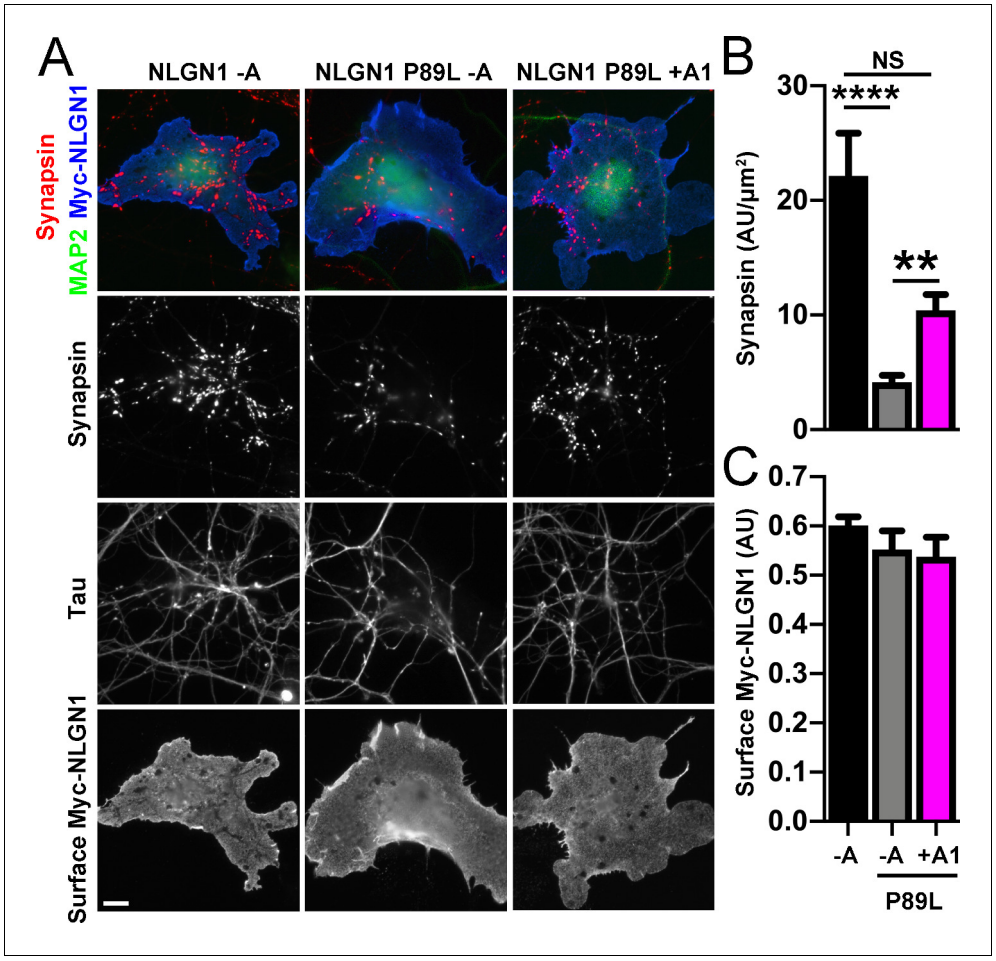

Figure 8. A1 splice inclusion in the autism-linked NLGN1 P89L mutant enhances presynaptic differentiation in coculture. (**A–C**) Myc-NLGN1 -A, Myc-NLGN1 P89L -A, or Myc-NLGN1 P89L +A1 was expressed in COS7 cells which were cocultured with hippocampal neurons. The total intensity of synapsin (**B**) per COS7 cell - axon contact area lacking contact with MAP2-positive dendrites was normalized to a baseline value of 1 measured from sister cocultures performed with the negative control protein Myc-tagged CD4. Synapsin clustering by NLGN1 -A was reduced by the P89L mutation and partially restored by A1 splice site inclusion, ****p<0.0001, **p<0.01, NS not significant by Kruskal-Wallis test with post hoc Dunn's multiple comparisons test. n = 18–29 cells from two independent experiments. COS7 cells were chosen for equal NLGN1 expression (**C**). Scale bar, 10 µm.

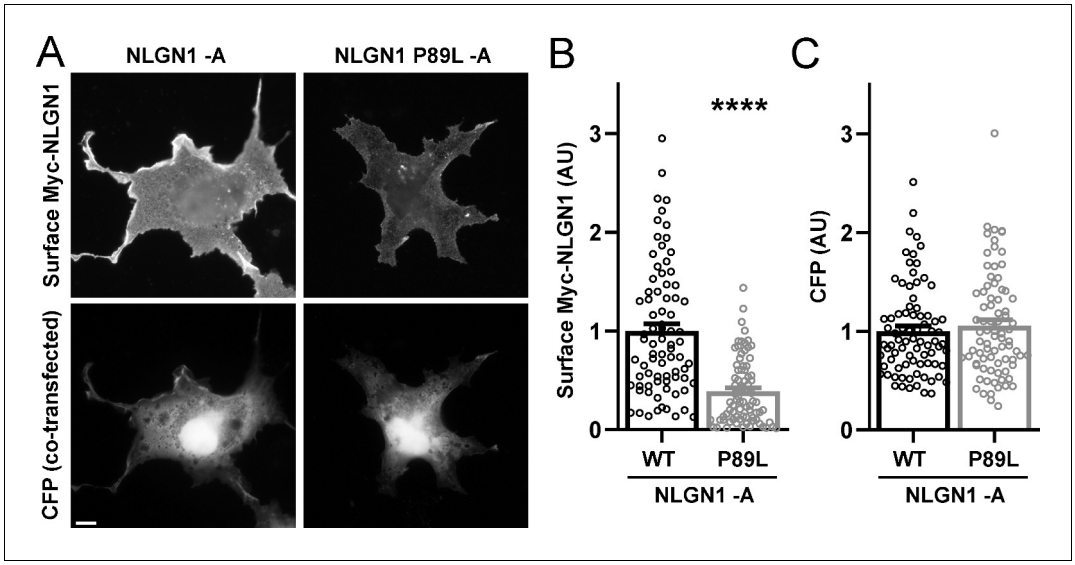

Figure 8—figure supplement 1. The NLGN1 P89L mutation reduces surface expression. COS7 cells were co-transfected with expression vectors for CFP and for Myc-NLGN1 -A (WT) or Myc-NLGN1 P89L -A. After 48 hr, cells were fixed without permeabilization and immunolabelled for surface Myc. Cells were chosen for imaging only by CFP expression. Myc-NLGN1 P89L -A showed reduced surface expression relative to WT, ****p<0.0001 by Mann-Whitney test, n = 80 cells from two independent experiments. Scale bar, 10 μm.

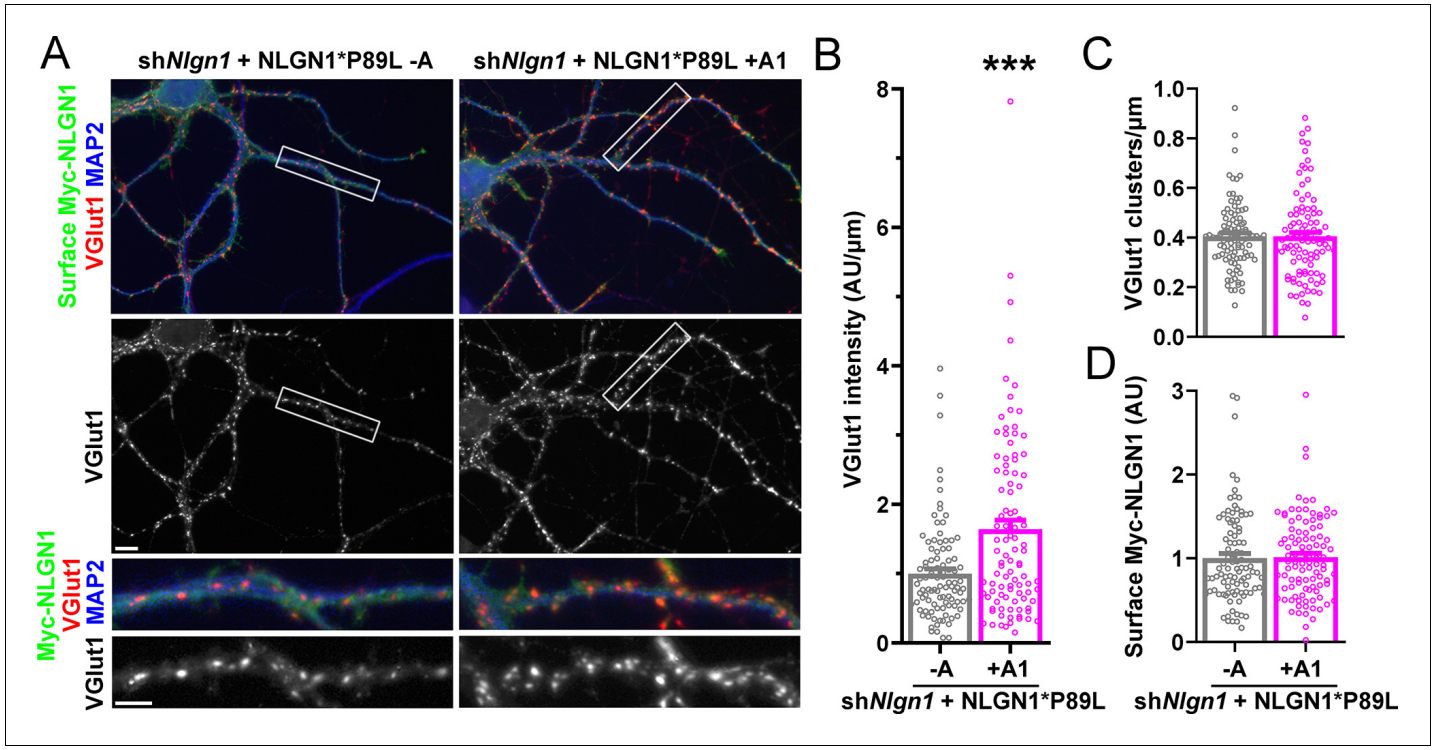

Figure 9. A1 splice inclusion in the autism-linked NLGN1 P89L mutant promotes synapse development. (**A–D**) Cultured hippocampal neurons were transfected with U6-sh*Nlgn1*-hSyn-YFP and hSyn-CFP-P2A-Myc-NLGN1* P89L -A or P89L +A1 at DIV 5 and neurons were fixed at DIV 13. The density of VGlut1 clusters did not differ (**C**) but the total fluorescence intensity of VGlut1 inputs (**B**) was higher for neurons expressing NLGN1* P89L +A1 than the -A isoform, ***p=0.0008 by Mann Whitney test, n = 97–99 neurons from three independent experiments. Cells were chosen by equal surface Myc-NLGN1 immunofluorescence (**D**). Scale bar, top 10 µm, bottom 5 µm.